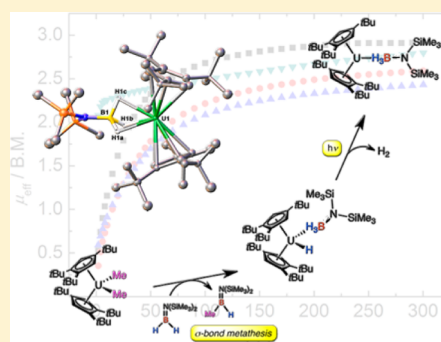


Uranium Hydridoborates: Synthesis, Magnetism, and X-ray/Neutron Diffraction Structures

H. Braunschweig,^{*,†} A. Gackstatter,[†] T. Kupfer,^{*,†} K. Radacki,[†] S. Franke,[‡] K. Meyer,[‡] K. Fucke,[§] and M.-H. Lemée-Cailleau^{||}[†]Institut für Anorganische Chemie, Julius-Maximilians-Universität Würzburg, Am Hubland, D-97074 Würzburg, Germany[‡]Institut für Chemie und Pharmazie, Anorganische Chemie, Friedrich-Alexander Universität Erlangen-Nürnberg, D-91058 Erlangen, Germany[§]School of Medicine, Pharmacy and Health, Durham University, Queen's Campus, University Boulevard, Stockton-on-Tees TS17 6BH, U.K.^{||}Institut Laue-Langevin, F-38042 Grenoble, France

S Supporting Information

ABSTRACT: While uranium hydridoborate complexes containing the $[\text{BH}_4]^-$ moiety have been well-known in the literature for many years, species with functionalized borate centers remained considerably rare. We were now able to prepare several uranium hydridoborates (**1–4**) with amino-substituted borate moieties with high selectivity by smooth reaction of $[\text{Cp}^*_2\text{UME}_2]$ ($\text{Cp}^* = \text{C}_5\text{Me}_5$) and $[\text{Cp}'_2\text{UME}_2]$ ($\text{Cp}' = 1,2,4\text{-}t\text{Bu}_3\text{C}_5\text{H}_2$) with the aminoborane $\text{H}_2\text{BN}(\text{SiMe}_3)_2$. A combination of nuclear magnetic resonance spectroscopy, deuteration experiments, magnetic SQUID measurements, and X-ray/neutron diffraction studies was used to verify the anticipated molecular structures and oxidation states of **1–4** and helped to establish a linear tridentate coordination mode of the borate anions.



INTRODUCTION

During the past several decades, research in the field of organometallic *f*-element chemistry has demonstrated that uranium hydridoborate complexes represent a unique class of metal compounds with highly interesting structural and magnetic properties.^{1,2} However, a closer look at the literature showed that this field is still strongly dominated by the $[\text{BH}_4]^-$ anion, which is at least in part related to experimental limitations in the synthesis of uranium borohydrides. For many years, most uranium borate species have been derived directly or indirectly from unsolvated $[\text{U}^{\text{IV}}(\text{BH}_4)_4]$, whose synthesis requires special equipment (vacuum vibration ball mill)³ and was thus not available to all researchers. Only very recently did Arnold et al. develop a new protocol for the high-yield synthesis of $[\text{U}^{\text{III}}(\text{BH}_4)_3(\text{THF})_2]$, which might allow a convenient entry into U^{III} borate chemistry in the future.⁴ Other methods for the introduction of the $[\text{BH}_4]^-$ ligand such as salt metathesis or BH_3 insertion reactions are known, but they have not found widespread application to far.^{1,2} For uranium borohydrides with different substitution patterns at boron, no general synthetic approach has been available to date, and the number of known complexes is comparably small.^{1,2} However, a fine-tuning of the electronic properties of the borate anion by selective functionalization would be highly desirable, because this is also expected to alter the reactivities of the hydridoborate complexes, which might clear the way for novel application ranges. Different strategies have sporadically

been used for the generation of the former, including (i) salt elimination,^{5–10} (ii) insertion of BH_3 into various $\text{U}-\text{X}$ bonds,^{11,12} and (iii) metathesis reactions of $[\text{BH}_4]^-$ complexes with BR_3 .^{5,13}

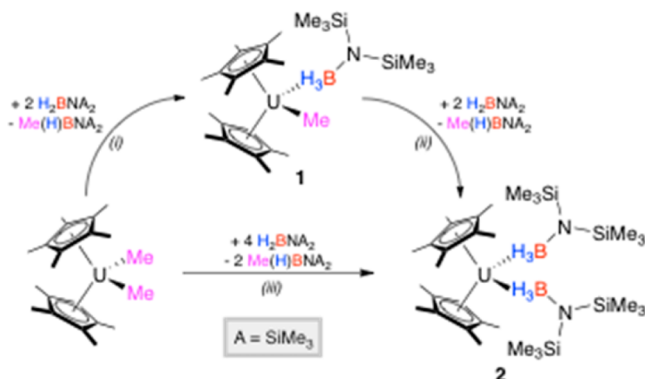
We were now able to establish the second approach as a convenient route for accessing uranium borohydride complexes (**1–4**) containing functionalized borate moieties with high selectivity by reaction of the methyl complexes $[\text{Cp}^*_2\text{UME}_2]$ ¹⁴ ($\text{Cp}^* = \text{C}_5\text{Me}_5$) and $[\text{Cp}'_2\text{UME}_2]$ ¹⁵ ($\text{Cp}' = 1,2,4\text{-}t\text{Bu}_3\text{C}_5\text{H}_2$) with aminoborane $\text{H}_2\text{BN}(\text{SiMe}_3)_2$. This method allows a facile alteration of the electronic properties of the borate ligand.

RESULTS AND DISCUSSION

We began our studies with the stoichiometric 1:1 reaction of $[\text{Cp}^*_2\text{UME}_2]$ and $\text{H}_2\text{BN}(\text{SiMe}_3)_2$ in benzene at room temperature. The reaction was fast and proceeded with high selectivity to afford hydridoborate complex **1** (Scheme 1). While consumption of $\text{H}_2\text{BN}(\text{SiMe}_3)_2$ was quantitative within minutes, ^1H nuclear magnetic resonance (NMR) spectroscopy indicated only 50% conversion of $[\text{Cp}^*_2\text{UME}_2]$. This finding was easily rationalized by ^{11}B NMR spectroscopy, which showed that only half of the aminoborane (δ 48.0) has been converted directly into uranium borate **1** (δ 207). Instead, the

Received: May 28, 2015

Published: August 6, 2015

Scheme 1. Synthesis of Hydridoborate Complexes 1 and 2^a

^aReaction conditions: (i) 2 equiv of H₂BN(SiMe₃)₂, C₆H₆, room temperature, 5 min; –(H)(Me)BN(SiMe₃)₂; (ii) 2 equiv of H₂BN(SiMe₃)₂, C₆H₆, room temperature, 2 h; –(H)(Me)BN(SiMe₃)₂; (iii) 4 equiv of H₂BN(SiMe₃)₂, C₆H₆, room temperature, 2 h; –2 equiv of (H)(Me)BN(SiMe₃)₂.

transformation is accompanied by the generation of 1 equiv of (H)(Me)BN(SiMe₃)₂ (δ 53). No intermediates are evident in the ¹H NMR and ¹¹B NMR spectra.

Addition of a second equivalent of H₂BN(SiMe₃)₂ to the reaction mixture resulted in the quantitative formation of hydridoborate 1, which was eventually isolated in 85% yield as an orange, crystalline solid after recrystallization from *n*-pentane. All analytical data [NMR spectroscopy, elemental analysis, SQUID, and X-ray diffraction (Figures 2 and 3)] are fully consistent with the description of 1 as a mixed methyl hydridoborate complex with uranium in the expected oxidation state of +IV. The presence of a U–Me moiety makes 1 much more thermally labile and sensitive to oxygen and moisture than the related hydridoborates 2–4.

Despite its paramagnetic nature, 1 shows surprisingly sharp signals at δ 8.74 (ω_{1/2} = 7.6 Hz), δ –12.56 (ω_{1/2} = 79.2 Hz), and δ –191.42 (ω_{1/2} = 70.5 Hz) in the ¹H NMR spectrum (C₆D₆) for the Cp*, SiMe₃, and Me protons, respectively (Table 1). By contrast, the ¹H NMR resonance that can be assigned to the bridging borate hydrogen atoms (δ –17) is considerably broader (ω_{1/2} = 265.4 Hz) and rather difficult to observe. As expected, this signal shows a quartet pattern; however, its large full width at half-maximum prevents any

extraction of a meaningful ¹J_{B–H} coupling constant. To exclude the presence of any additional U–H bonds and to facilitate the detection of hydrogen atoms introduced into the hydridoborate products by the aminoborane, we also prepared the deuterium-labeled analogue [Cp*₂U(Me){D₃BN(SiMe₃)₂}] (1_D) by reaction of [Cp*₂U(OMe)₂] and D₂BN(SiMe₃)₂. Here, reaction times are a bit longer than for 1, but 1_D is also formed quantitatively within 10 min at room temperature (RT) in benzene (78% isolated yield). As expected for 1_D, only one resonance is evident in the ²D NMR spectrum in C₆H₆ (δ –16.3; ω_{1/2} = 29.4 Hz), which becomes significantly sharper upon ¹¹B decoupling (ω_{1/2} = 22.0 Hz), thus further verifying its assignment. Interestingly, the ¹¹B NMR resonance of 1_D (δ 213) is shifted to lower field by 6 ppm upon deuteration of the borate moiety (cf. 1, δ 207). As shown below, this shift is a general feature of the partially deuterated hydridoborate species and is also observed for complexes 2–4 [see below (Table 1)].

Addition of an additional 2 equiv of H₂BN(SiMe₃)₂ to benzene solutions of 1 causes the replacement of the second methyl group with a borate moiety with concomitant formation of hydridoborate 2 and 1 equiv of (H)(Me)BN(SiMe₃)₂ (Scheme 1). However, considerably longer reaction times (2 h) are required for complete conversion of 1 into 2, which is most likely related to the increased level of steric protection of the U–Me bond. Similarly, the deuterium-labeled analogue [Cp*₂U{D₃BN(SiMe₃)₂}] (2_D) readily formed upon treatment of 1_D with D₂BN(SiMe₃)₂. Both species were isolated as orange, crystalline solids in excellent yields of 87% (2) and 81% (2_D) after recrystallization from *n*-pentane solutions at –30 °C. The presence of two borate ligands in the coordination sphere of uranium +IV centers in 2 and 2_D is clearly verified by magnetic SQUID measurements (Figure 2) and X-ray diffraction studies (Figure 3), as well as NMR spectroscopy and elemental analyses.

Accordingly, the ¹H NMR spectrum of 2 features three paramagnetically shifted resonances at δ 11.12 (Cp*; ω_{1/2} = 4.7 Hz), δ –9.67 (SiMe₃; ω_{1/2} = 9.1 Hz), and δ –39 (H₃B; ω_{1/2} = 550.3 Hz) with a relative integration ratio of 30:36:6 (Table 1). As already noted for 1 and 1_D, the bridging borate hydrogen atoms of 2 appear as a very broad signal in the ¹H NMR spectrum (ω_{1/2} = 550.3 Hz), while the corresponding ²D NMR resonance of 2_D (δ –39.8) possesses a significantly smaller line width (ω_{1/2} = 37.3 Hz), which becomes even smaller upon ¹¹B

Table 1. NMR Spectroscopic Data of Hydridoborates 1–4 and 1_D–4_D^a

	¹ H NMR (δ, RT) ^b				² D NMR (δ, RT) ^c		¹¹ B NMR (δ, RT) ^b
	C ₅ (CH ₃) ₅	^t Bu ₃ C ₅ H ₂	^t Bu ₃ C ₅ H ₂	Si(CH ₃) ₃	H ₃ B-	D ₃ B- U-D	
1	8.74 (7.6)			–12.56 (79.2)	–17 (265.4)		207 (162.9)
1 _D						–16.3 (29.4)	213 (69.4)
2	11.12 (4.7)			–9.67 (9.1)	–39 (550.3)		154 (167.6)
2 _D						–39.8 (37.3)	159 (73.4)
3		13.8, 3.1, –2.8, –16.6, –18.9 (1200–1600) ^d		–10.99 (76.8)	22 (848.0) ^e		231 (257.7)
3 _D						22.6 (47.4) 327.9 (29.5)	237 (156.0)
4		0.75 (38.7) –1.80 (10.4) –4.09 (22.0)	50.30 (67.8)	–29.73 (35.2)	196 (349.2)		261 (137.2)
4 _D						197.6 (34.2)	273 (84.3)

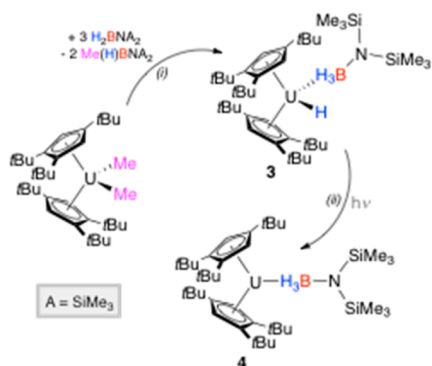
^aChemical shifts (δ) are given in parts per million. Values in parentheses are the full widths at half-maximum, ω_{1/2} (in hertz). ^bIn C₆D₆. ^cIn C₆H₆.

^dResonances are very broad and hard to assign and integrate reliably. ^eThe ¹H NMR resonance of the uranium-bound hydride U–H is not observed at room temperature.

decoupling ($\omega_{1/2} = 24.6$ Hz). One single ^{11}B NMR resonance is found for both **2** (δ 154) and **2_D** (δ 159), which is once again shifted to lower field by 5 ppm for partially deuterated **2_D**. Hydridoborates **2** and **2_D** are also readily obtained in one step directly from $[\text{Cp}^*_2\text{U}\text{Me}_2]$ by reaction with 4 equiv of the respective aminoborane in a benzene solution. Here, 2 equiv of the side product $(\text{H}/\text{D})(\text{Me})\text{BN}(\text{SiMe}_3)_2$ is formed during the transformation, while isolated yields remain almost identical.

Next, we studied the impact of the sterics on the reaction rates and products by reacting the bulky uranium methyl complex $[\text{Cp}'_2\text{U}\text{Me}_2]$ with 2 equiv of $\text{H}_2\text{BN}(\text{SiMe}_3)_2$ in benzene (Scheme 2). Here, a different reactivity pattern was

Scheme 2. Synthesis of Hydridoborate Complexes **3** and **4**^a



^aReaction conditions: (i) 3 equiv of $\text{H}_2\text{BN}(\text{SiMe}_3)_2$, C_6H_6 , RT, 24 h; -2 equiv of $(\text{H})(\text{Me})\text{BN}(\text{SiMe}_3)_2$; (ii) $h\nu$, C_6H_6 , RT, 20 h; $-1/2\text{H}_2$.

observed, and much longer reaction times (24 h) were required for complete consumption of the aminoborane. According to ^{11}B NMR spectroscopy, the hydridoborate $[\text{Cp}'_2\text{U}(\text{H})\{\text{H}_3\text{BN}(\text{SiMe}_3)_2\}]$ (**3**; δ 231) is generated with high selectivity along with $(\text{H})(\text{Me})\text{BN}(\text{SiMe}_3)_2$ as a side product. However, **3** and $(\text{H})(\text{Me})\text{BN}(\text{SiMe}_3)_2$ are not formed in a 1:1 ratio as found for the $[\text{Cp}^*_2\text{U}\text{Me}_2]$ system, but in a relative ratio of 1:2. In addition, ^1H NMR spectroscopy clearly indicated the presence of unreacted $[\text{Cp}'_2\text{U}\text{Me}_2]$ in the reaction mixture. Thus, a third equivalent of $\text{H}_2\text{BN}(\text{SiMe}_3)_2$ was necessary for quantitative conversion into **3**, which was isolated as red crystals in 76% yield after recrystallization from *n*-pentane. Initially, the exact nature of **3** remained unclear, because the presence of a uranium-bound hydride ligand was not evident from NMR spectroscopic and X-ray diffraction data (Figure 3). The ^1H NMR spectrum of **3** did not reveal much structural information and features only very broad resonances [$\omega_{1/2} = 800\text{--}1600$ Hz (Table 1)]. Only the ^1H NMR signal of the SiMe_3 groups could be identified without any doubt (δ -10.99 ; $\omega_{1/2} = 76.8$ Hz), while the other resonances could not be assigned unequivocally (Cp ring, borate) or were not observed at room temperature at all (Cp ring/hydride). On the other hand, the results of an X-ray diffraction study of **3** (Figure 3) were rather misleading, because the large atomic number of uranium efficiently hampers the localization of any directly attached hydride ligands. Accordingly, only the main structural features of **3** are reflected by X-ray diffraction, thus suggesting a U(III) borate species.

This puzzle was finally solved by subsequent magnetic SQUID measurements (Figure 2) and deuteration experiments. Thus, SQUID revealed the presence of a uranium center in the +IV oxidation state, which is why hydridoborate **3** must contain

an additional ligand in the coordination sphere of uranium. Along with the results of the aforementioned X-ray diffraction study, a uranium-bound hydride ligand appeared to be most reasonable. However, because we were not able to verify this by ^1H NMR spectroscopy, the partially deuterated analogue $[\text{Cp}'_2\text{U}(\text{D})\{\text{D}_3\text{BN}(\text{SiMe}_3)_2\}]$ **3_D** was prepared by reaction of $[\text{Cp}'_2\text{U}\text{Me}_2]$ with 3 equiv of $\text{D}_2\text{BN}(\text{SiMe}_3)_2$ in 81% isolated yield. Two distinct resonances were visible in the ^2D NMR spectrum of **3_D** (C_6H_6). The ^2D NMR signal at δ 22.6 ($\omega_{1/2} = 47.4$ Hz; $^2\text{D}\{^{11}\text{B}\}$ NMR, $\omega_{1/2} = 37.1$ Hz) could easily be assigned to the bridging borate deuterium atoms. The corresponding signal for the bridging hydrides in **3** was also present in its ^1H NMR spectrum (δ 22; $\omega_{1/2} = 848.0$ Hz). By contrast, the second ^2D NMR resonance of **3_D** does not have a ^1H NMR counterpart for **3**. This signal is detected at extremely low frequencies at δ 327.9 ($\omega_{1/2} = 29.5$ Hz) and clearly corresponds to the uranium-bound deuteride, thus eventually clarifying the identity of **3** and **3_D**.

Irradiation of benzene solutions of **3** and **3_D** is accompanied by the loss of H_2/D_2 and the selective formation of hydridoborates **4** and **4_D**, respectively (Scheme 2). The reactions can readily be tracked by ^{11}B NMR spectroscopy of the reaction mixtures (Table 1), which indicated the gradual consumption of **3** (δ 231) and **3_D** (δ 237) and the appearance of new ^{11}B NMR resonances for **4** (δ 261; $\omega_{1/2} = 137.2$ Hz) and **4_D** (δ 273; $\omega_{1/2} = 84.3$ Hz). Quantitative conversion is reached after irradiation for 24 h, while no boron-containing intermediates or side products can be detected during these redox processes. Both species are isolated in excellent yields (**4**, 88%; **4_D**, 74%) as dark red crystals after recrystallization from *n*-pentane at -30°C .

By contrast to that of **3**, the ^1H NMR spectrum of **4** features rather sharp resonances at δ 50.30 (4H; $\omega_{1/2} = 67.8$ Hz), δ 0.75 (18H; $\omega_{1/2} = 38.7$ Hz), δ -1.80 (18H; $\omega_{1/2} = 10.5$ Hz), and δ -4.09 (18H; $\omega_{1/2} = 67.8$ Hz) for the Cp' ligand, and at δ -29.73 (18H; $\omega_{1/2} = 39.2$ Hz) for the SiMe_3 groups (Table 1). The bridging hydrides of the borate moiety are observed as a broad signal at δ 196 (3H; $\omega_{1/2} = 349.2$ Hz). No signs for additional resonances that can be assigned to a uranium-bound hydride ligand are present, which is further supported by the ^2D NMR spectrum of the deuterated analogue $[\text{Cp}'_2\text{U}\{\text{D}_3\text{BN}(\text{SiMe}_3)_2\}]$ (**4_D**). Only a single ^2D NMR resonance is found with a chemical shift of δ 197.6 ($\omega_{1/2} = 34.2$ Hz; $^2\text{D}\{^{11}\text{B}\}$ NMR, $\omega_{1/2} = 22.0$ Hz). Moreover, the loss of the uranium-bound hydride/deuteride ligand in **3** and **3_D** is directly associated with the reduction of the uranium center to +III in borate products **4** and **4_D**, respectively, which was clearly verified by magnetic SQUID measurements (Figure 2).

However, the most convincing proof of the lack of any additional U–H bonds comes from a neutron diffraction study of single crystals of **4**, which ultimately legitimates its formulation as a U(III) hydridoborate complex (Figure 1). Crystals suitable for neutron diffraction were grown from saturated *n*-pentane solutions of **4** at -30°C . A diffraction data set was collected on VIVALDI at the Institute Laue Langevin in Grenoble, France. Though the crystals were rather small, the refined neutron diffraction structure definitely verifies the anticipated molecular structure of **4**. Thus, the existence of three hydrogen atoms in a bridging position between boron and uranium is clearly identified, proving an almost symmetrical tridentate coordination mode of the borate anion to a uranium center in the +III oxidation state. No additional uranium-bound

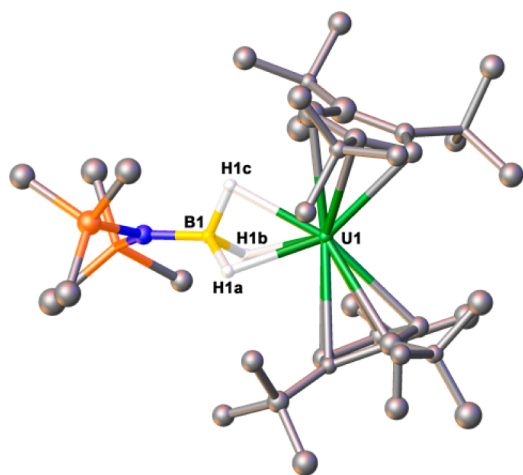


Figure 1. Neutron diffraction structure of **4**. Color code: carbon, gray; hydrogen, white; nitrogen, blue; silicon, orange; boron, yellow; uranium, green. Hydrogen atoms except for those bound to boron have been omitted for the sake of clarity.

hydrogen atoms are present in the neutron diffraction structure of **4**.

MAGNETIC PROPERTIES

Variable-temperature (2–300 K) SQUID magnetization measurements were used to provide a more detailed picture of the magnetic properties and the electronic structures of hydridoborate complexes **1–4** and to eventually verify their formal oxidation state (Figure 2). Thus, uranium borates **1–3**

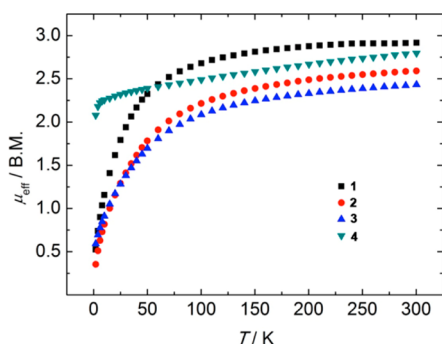


Figure 2. Temperature-dependent SQUID magnetization data of complexes **1** (black), **2** (red), **3** (blue), and **4** (gray) as a plot of μ_{eff} vs T . Data were corrected for underlying diamagnetism. Reproducibility was checked from at least two independently synthesized and measured samples.

possess RT magnetic moments of 2.92, 2.59, and 2.43 μ_{B} , respectively, that decrease to 0.53, 0.35, and 0.59 μ_{B} , respectively, at 2 K. These observations are in excellent agreement with the formulation of tetravalent uranium centers with their distinctive nonmagnetic $^3\text{H}_4$ ground state at low temperatures.¹⁶ By contrast, **4** exhibits a RT magnetic moment of 2.80 μ_{B} that decreases to 2.08 μ_{B} at 2 K.

The observed magnetic moments and their temperature dependency are typical for trivalent complexes of uranium with an f^3 electron configuration, a $^4\text{I}_{9/2}$ term, and a low-temperature doublet ground state.

X-RAY DIFFRACTION STRUCTURES

The molecular structures of hydridoborates **1–4**¹⁷ have also been assessed by X-ray diffraction studies (Figure 3). Relevant structural parameters are listed in Table 2. In all cases, the hydrogen atoms attached to the boron and uranium centers could not be located on the Fourier maps. Consequently, we determined their geometric positions by density functional theory (DFT) calculations¹⁸ and subsequently included them in the refinement using calculated U–H (borate, 2.27 Å; hydride, 1.96 Å), B–H (borate, 1.27 Å), and H–H (borate, 1.95 Å) distances. Overall, X-ray diffraction supports the molecular compositions of **1–4** as suggested by NMR spectroscopy and magnetic SQUID measurements.

The geometrical parameters for the four molecular structures are similar to each other. Thus, the averaged U–C(Cp) bond lengths to the η^5 -coordinated Cp ligands lie within a close range from 2.73 to 2.797(5) Å [absolute U–C(Cp) values of 2.667(8)–2.851(5) Å], which is comparable to the values found for related uranium species.^{15,21–25} Similarly, values for the U–Cp^{cent} distances (2.47–2.52 Å) and Cp^{cent}–U–Cp^{cent} angles (129.2–141.3°) in **1–4** strongly resemble those of other known Cp₂U-based species.^{15,21–25} The steric requirements of the ring substituents force the two Cp rings of **1–4** to adopt staggered conformations (torsion angles between 25.6° and 45.8°), while the arrangement of the Cp' rings in **3** and **4** is also influenced by steric repulsion of the bulky *t*Bu and N(SiMe₃)₂ groups.

With respect to the borate moieties, almost linear U–B–N bond angles [174.6(8)–178.6(8)°] in combination with the results obtained by neutron diffraction and DFT calculations clearly indicate a symmetric tridentate coordination mode of the borate ligand with three bridging hydrogen atoms in all hydridoborate complexes. The U–B bond lengths of **1–4** differ only marginally [2.494(11)–2.632(11) Å] and fall within the typical range observed in uranium borate species (2.45–2.78 Å).¹⁴ In addition, the U–C distances for the uranium methyl linkage in **1** [U1–C1, 2.435(9) Å; U2–C2, 2.394(10) Å; U3–C3, 2.461(10) Å] are very similar to those found for instance in [Cp'₂UME₂] [2.37(3) Å].¹⁵

CONCLUSIONS

In this work, we present a highly selective approach to the synthesis of uranium hydridoborates containing a substituted borate backbone. However, the nature of the reaction products depended on both the steric requirements of the Cp ring substituents and the reaction stoichiometry. Thus, the reactivity of the Cp*-based system was straightforward, and reaction of [Cp*₂UME₂] with 2 and 4 equiv of H₂BN(SiMe₃)₂ smoothly afforded methyl hydridoborate **1** and bis(borate) **2**, respectively. By contrast, the sterics of the more bulky Cp' system allowed for the introduction of only one borate ligand, and 3 equiv of H₂BN(SiMe₃)₂ was required to quantitatively yield hydridoborate **3**. However, a combination of NMR spectroscopic studies, deuteration experiments, and magnetic SQUID measurements was necessary to eventually verify the presence of one additional hydride ligand at the uranium(IV) center of **3**. Irradiation of this species subsequently resulted in the reduction of the uranium center with concomitant H₂ elimination, and generation of U(III) borate complex **4**. In all cases, X-ray and neutron diffraction data indicated that the borate ligand adopts a linear tridentate coordination mode with three bridging hydrogen atoms. With these results in mind, we

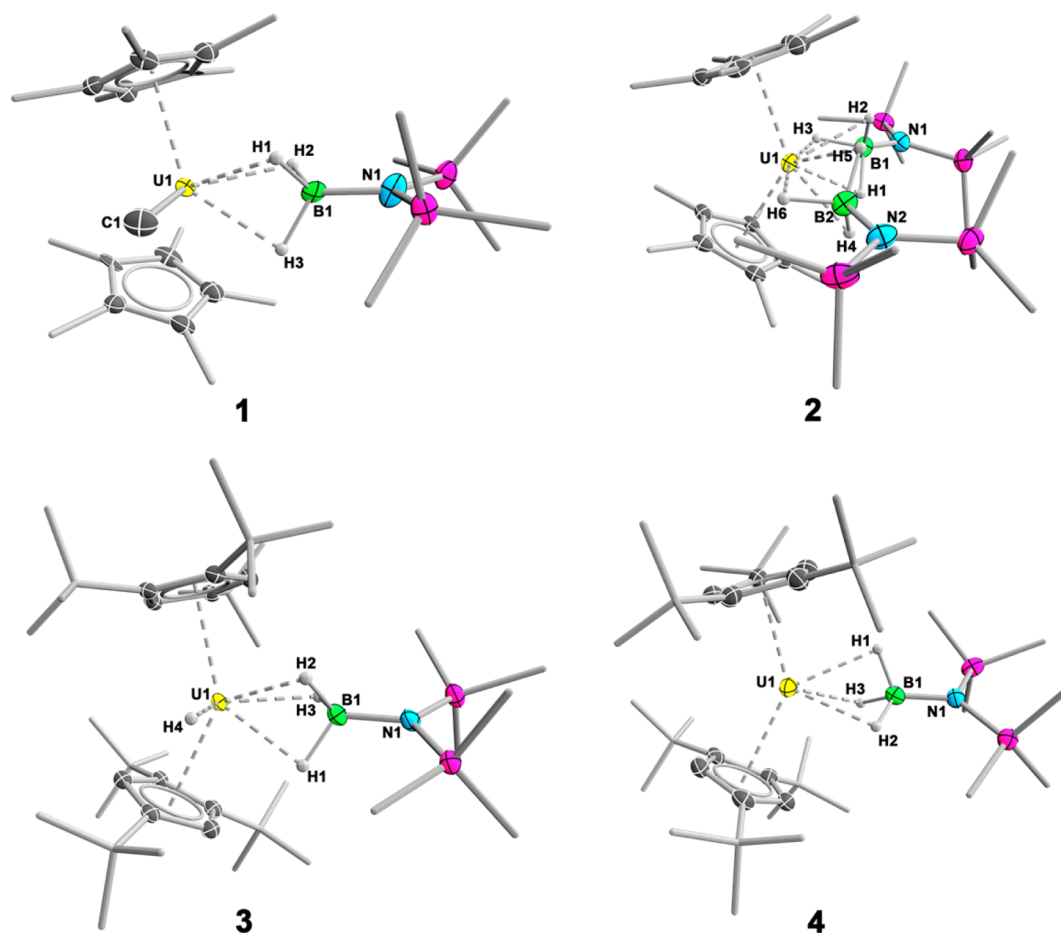


Figure 3. Molecular structures of hydridoborates 1–4 in the solid state determined by X-ray diffraction. Only one independent molecule of 1 is depicted. For the sake of clarity, ellipsoids of the ring substituents and the SiMe₃ groups as well as the disorder in 2 are not shown, and only hydrogen atoms directly attached to uranium and boron are displayed. Relevant bond distances and angles are listed in Table 2.

Table 2. Selected Distances (angstroms) and Angles (degrees) of Hydridoborates 1–4

	C(Cp)···U (av)	C(Cp)···U (range)	Cp ^{cent} ···U (av)	Cp ^{cent} –U–Cp ^{cent}	U–B	U–B–N	U–C(Me)
1 ^a	2.736(9)	2.667(8) 2.827(9)	2.47	135.8 135.6 133.4	2.564(11) 2.632(12) 2.494(11)	174.6(8) 177.9(7) 178.6(8)	2.435(9) 2.394(10) 2.461(10)
2 ^b	2.73	2.68 2.80	2.50	129.2	B1 2.555(4) B2 2.562(4)	B1 175.6 B2 177.0	
3	2.776(3)	2.730(3) 2.828(3)	2.50	141.3	2.545(4)	177.6(3)	
4	2.797(5)	2.751(5) 2.851(5)	2.52	140.1	2.580(6)	177.6(4)	

^aThree independent molecules are present in the asymmetric unit of 1. ^bThe molecular structure of 2 shows a strong disorder of both Cp* and borate ligands. Thus, averaged values are provided.

now aim at a generalization of this approach by varying the substituents at the boron reagent, i.e., different amine groups or substitution of the amine functionality by alkyl/aryl moieties. The results of these studies will be reported in the near future.

EXPERIMENTAL SECTION

General Remarks. All manipulations were performed under an atmosphere of dry argon using standard Schlenk line or glovebox techniques. Solvents were purified by distillation from appropriate drying agents and degassed immediately prior to use. C₆D₆ was degassed by three freeze–pump–thaw cycles and stored over molecular sieves. [Cp*₂UMe₂],¹⁴ [Cp*₂UMe₂],¹⁵ and H₂BN(SiMe₃)₂²⁶ were prepared according to literature procedures. NMR spectra were

acquired on a Bruker Avance 500 FT-NMR spectrometer. NMR spectra were referenced to external SiMe₄ (¹H, ²D, and ¹³C), and BF₃·OEt₂ (¹¹B). Microanalyses (C, H, N) were performed on a Leco Instruments analyzer, type CHNS 932. A Hg/Xe arc lamp (400–550 W) equipped with IR filters irradiating at 210–600 nm was used as a light source during photolysis experiments.

D₂BN(SiMe₃)₂. A flask was charged with Bu₃SnD (10 g, 34.2 mmol), and the contents were treated with Cl₂BN(SiMe₃)₂ (4.33 g, 17.9 mmol) at room temperature. The reaction mixture was then heated at 45 °C over a period of 2 h. D₂BN(SiMe₃)₂ (1.88 g, 10.7 mmol, 60%) was isolated by vacuum distillation from the reaction mixture (40 °C, 10 mbar) as a colorless, pyrophoric liquid: ¹H NMR (C₆D₆, RT) δ 0.18 (s, 18H, SiMe₃); ²D NMR (C₆H₆, RT) δ 5.1 (s,

D₂B-); ¹¹B NMR (C₆D₆, RT) δ 48. El. Anal. Calcd for C₆H₁₈D₂BNSi₂: C, 41.13; H, 12.65; N, 7.99. Found: C, 40.88; H, 12.83; N, 8.18.

1. In a glovebox, H₂BN(SiMe₃)₂ (0.81 g, 4.64 mmol) was added dropwise to a stirred solution of [Cp*₂UMe₂] (1.25 g, 2.32 mmol) in benzene (10 mL). After 10 min, all volatiles were removed *in vacuo*. Subsequently, the residue was extracted into *n*-pentane (25 mL), and all insoluble components were removed by filtration. The filtrate was reduced in volume to ~7 mL and stored at –30 °C to afford 1 (1.38 g, 1.97 mmol, 85%) as orange needles: ¹H NMR (C₆D₆, RT) δ –191.42 (s, 3H, U-Me), –17 (s, 3H, H₃B-), –12.56 (s, 18H, SiMe₃), 8.74 (s, 30H, Cp*); ¹¹B NMR (C₆D₆, RT) δ 207. El. Anal. Calcd for C₂₇H₅₄BNSi₂U: C, 46.48; H, 7.80; N, 2.01. Found: C, 46.47; H, 7.75; N, 1.95.

1_D. Deuterium-labeled 1_D (0.57 g, 0.81 mmol, 78%) was prepared according to the method described for 1 using [Cp*₂UMe₂] (0.56 g, 1.04 mmol) and D₂BN(SiMe₃)₂ (0.36 g, 2.08 mmol): ²D NMR (C₆H₆, RT) δ –16.3 (s, D₂B-); ¹¹B NMR (C₆D₆, RT) δ 213.

2. Method a. A solution of 1 (0.50 g, 0.72 mmol) in benzene (10 mL) was treated dropwise with H₂BN(SiMe₃)₂ (0.25 g, 1.43 mmol) at room temperature. The reaction mixture was allowed to stir for 2 h, after which time all volatiles were removed *in vacuo*. The residue was extracted into *n*-pentane (20 mL); all insoluble components were removed by filtration, and the filtrate was reduced in volume to ~5 mL. Storage at –30 °C yielded 2 (0.54 g, 0.63 mmol, 87%) as an orange, crystalline solid: ¹H NMR (C₆D₆, RT) δ –191.42 (s, 3H, U-Me), –39 (s, 6H, H₃B-), –9.67 (s, 36H, SiMe₃), 11.12 (s, 30H, Cp*); ¹¹B NMR (C₆D₆, RT) δ 154. El. Anal. Calcd for C₃₂H₇₂B₂N₂Si₄U: C, 44.85; H, 8.47; N, 3.27. Found: C, 44.69; H, 8.24; N, 3.05.

2. Method b. A flask was charged with [Cp*₂UMe₂] (0.53 g, 0.98 mmol) in benzene (10 mL). H₂BN(SiMe₃)₂ (0.68 g, 3.94 mmol) was added at room temperature, and the reaction mixture was allowed to stir for 2 h. All volatiles were removed *in vacuo*, and the residue was extracted into *n*-pentane (10 mL). Insoluble components were removed by filtration, and the filtrate was reduced in volume to ~3 mL. Storage at –30 °C afforded 2 (0.65 g, 0.75 mmol, 77%) as an orange, crystalline solid.

2_D. Deuterium-labeled 2_D (0.32 g, 0.37 mmol, 81%) was prepared according to method b described for 2 using [Cp*₂UMe₂] (0.25 g, 0.46 mmol) and D₂BN(SiMe₃)₂ (0.33 g, 1.86 mmol): ²D NMR (C₆H₆, RT) δ –16.3 (s, D₂B-); ¹¹B NMR (C₆D₆, RT) δ 213.

3. H₂BN(SiMe₃)₂ (0.71 g, 4.08 mmol) was added dropwise to a solution of [Cp*₂UMe₂] (1.00 g, 1.36 mmol) in benzene (20 mL). Subsequently, the reaction mixture was stirred at room temperature over a period of 24 h in the dark. After that time, all volatiles were removed *in vacuo*, and the residue was extracted into *n*-pentane (30 mL). After filtration, the filtrate was reduced in volume to ~10 mL and stored at –30 °C to afford 3 (0.91 g, 1.03 mmol, 76%) as a red, crystalline solid: ¹H NMR (C₆D₆, RT) δ –18.9, –16.6, –2.8, 3.1, 13.8 (all broad s), –10.99 (s, 18H, SiMe₃), 22 (s, 3H, H₃B-); ¹¹B NMR (C₆D₆, RT) δ 231. El. Anal. Calcd for C₄₀H₈₀BNSi₂U: C, 54.59; H, 9.16; N, 1.59. Found: C, 54.42; H, 8.93; N, 1.59.

3_D. Deuterium-labeled 3_D (0.59 g, 0.67 mmol, 81%) was prepared according to the method described for 3 using [Cp*₂UMe₂] (0.61 g, 0.83 mmol) and D₂BN(SiMe₃)₂ (0.44 g, 2.49 mmol): ²D NMR (C₆H₆, RT) δ 22.6 (s, D₂B-), 327.9 (s, U-D); ¹¹B NMR (C₆D₆, RT) δ 217.

4. A stirred solution of 3 (0.44 g, 0.50 mmol) in benzene (15 mL) was irradiated by a Hg/Xe arc lamp over a period of 24 h. Subsequently, all volatiles were removed *in vacuo*, and the residue was extracted into *n*-pentane (15 mL). Removal of insoluble components by filtration and storage at –30 °C yielded 4 (0.39 g, 0.44 mmol, 88%) as dark red blocks: ¹H NMR (C₆D₆, RT) δ –29.73 (s, 18H, SiMe₃), –4.09 (s, 18H, C₅H₂tBu₃), –1.80 (s, 18H, C₅H₂tBu₃), 0.75 (s, 18H, C₅H₂tBu₃), 50.30 (s, 4H, C₅H₂tBu₃), 196 (s, 3H, H₃B-); ¹¹B NMR (C₆D₆, RT) δ 261. El. Anal. Calcd for C₄₀H₇₉BNSi₂U: C, 54.65; H, 9.06; N, 1.59. Found: C, 54.61; H, 9.18; N, 1.59.

4_D. Deuterium-labeled 4_D (0.18 g, 0.21 mmol, 74%) was prepared according to the method described for 4 using 3_D (0.25 g, 0.28 mmol): ²D NMR (C₆H₆, RT) δ 197.6 (s, D₂B-); ¹¹B NMR (C₆D₆, RT) δ 273.

SQUID Measurements. Magnetism data of crystalline powdered samples (20–30 mg) were recorded with a SQUID magnetometer

(Quantum Design) at 10 kOe (2–300 K). Values of magnetic susceptibility were corrected for the underlying diamagnetic increment [χ_{dia} values of $-390.33 \times 10^{-6} \text{ cm}^3 \text{ mol}^{-1}$ (2), $-505.78 \times 10^{-6} \text{ cm}^3 \text{ mol}^{-1}$ (2), $-547.44 \times 10^{-6} \text{ cm}^3 \text{ mol}^{-1}$ (3), and $-517.45 \times 10^{-6} \text{ cm}^3 \text{ mol}^{-1}$ (4)] by using tabulated Pascal constants and the effect of the blank sample holders (gelatin capsule/straw).²⁷ Samples used for magnetization measurements were recrystallized multiple times and checked for chemical composition and purity by elemental analysis (C, H, and N) and NMR spectroscopy.

Crystallography. Crystallographic data have been deposited with the Cambridge Crystallographic Data Center as supplementary publications CCDC-1053163 (1), CCDC-1053164 (2), CCDC-1053165 (3), CCDC-1053162 (4, X-ray diffraction), and CCDC-1053166 (4, neutron diffraction). These data can be obtained free of charge from The Cambridge Crystallographic Data Centre via www.ccdc.cam.ac.uk/data_request/cif.

■ ASSOCIATED CONTENT

Supporting Information

The Supporting Information is available free of charge on the ACS Publications website at DOI: 10.1021/acs.inorgchem.5b01205.

Details of the crystal structure determinations and NMR spectra for all compounds (PDF)

■ AUTHOR INFORMATION

Corresponding Authors

*E-mail: h.braunschweig@uni-wuerzburg.de.

*E-mail: thomas.kupfer@uni-wuerzburg.de.

Notes

The authors declare no competing financial interest.

■ ACKNOWLEDGMENTS

We acknowledge generous financial support from the Deutsche Forschungsgemeinschaft (DFG).

■ REFERENCES

- (1) Ephritikhine, M. *Chem. Rev.* **1997**, 97, 2193–2242.
- (2) Makhaev, V. D. *Russ. Chem. Rev.* **2000**, 69, 727–746.
- (3) Volkov, V. V.; Myakishev, K. G. *Radiokhimiya* **1980**, 22, 745–749.
- (4) Arnold, P. L.; Stevens, C. J.; Farnaby, J. H.; Gardiner, M. G.; Nichol, G. S.; Love, J. B. *J. Am. Chem. Soc.* **2014**, 136, 10218–10221.
- (5) Marks, T. J.; Kolb, J. R. *J. Am. Chem. Soc.* **1975**, 97, 27–33.
- (6) Zanella, P.; Ossola, F.; Porchia, M.; Rossetto, G.; Chiesi Villa, A.; Guastini, C. *J. Organomet. Chem.* **1987**, 323, 295–303.
- (7) Blake, P. C.; Lappert, M. F.; Taylor, R. G.; Atwood, J. L.; Hunter, W. E.; Zhang, H. *J. Chem. Soc., Dalton Trans.* **1995**, 3335–3341.
- (8) Daly, S. R.; Girolami, G. S. *Chem. Commun.* **2010**, 46, 407–408.
- (9) Daly, S. R.; Girolami, G. S. *Inorg. Chem.* **2010**, 49, 5157–5166.
- (10) Mansell, S. M.; Bonnet, F.; Visseaux, M.; Arnold, P. *Dalton Trans.* **2013**, 42, 9033–9039.
- (11) Rossetto, G.; Porchia, M.; Ossola, F.; Zanella, P.; Fischer, R. D. *J. Chem. Soc., Chem. Commun.* **1985**, 1460–1461.
- (12) Porchia, M.; Brianese, N.; Ossola, F.; Rossetto, G.; Zanella, P. *J. Chem. Soc., Dalton Trans.* **1987**, 691–694.
- (13) Schlesinger, H. I.; Brown, H. C.; Horvitz, L.; Bond, A. C.; Tuck, L. D.; Walker, A. O. *J. Am. Chem. Soc.* **1953**, 75, 222–224.
- (14) Fagan, P. J.; Manriquez, J. M.; Maatta, E. A.; Seyam, A. M.; Marks, T. J. *J. Am. Chem. Soc.* **1981**, 103, 6650–6667.
- (15) Zi, G.; Jia, L.; Werkema, E. L.; Walter, M. D.; Gottfriedsen, J. P.; Andersen, R. A. *Organometallics* **2005**, 24, 4251–4264.
- (16) Siddall, T. H. *Theory and Applications of Molecular Paramagnetism*; Bundreaux, E. A., Mulay, L. N., Eds.; John Wiley and Sons: New York, 1976.

(17) **1** contains three independent molecules in the asymmetric unit. However, their structural parameters differ only marginally, which is why only one of the molecular structures is considered in the discussion. The molecular structure of **2** features a high degree of disorder for both the Cp* rings, and the two borate moieties. Consequently, structural parameters cannot be discussed.

(18) The geometric positions of the hydridic hydrogen atoms were determined as follows. First, hydrogen atoms of the borate groups were placed at idealized, tetrahedral positions in SHELXL. Next, only the positions of the relevant hydrogen atoms were optimized by DFT calculations [Turbomole; B3LYP/def2-SV(P); U: def-SV(P)/def-ecp]^{19,20} using X-ray diffraction coordinates as input geometry, and keeping all other atoms fixed at these positions.

(19) Ahlrichs, R.; et al. *Turbomole*, version 6.2; Turbomole GmbH: Karlsruhe, Germany, 2010.

(20) Weigend, F.; Ahlrichs, R. *Phys. Chem. Chem. Phys.* **2005**, *7*, 3297. Def2-SVP basis sets were obtained from the Extensible Computational Chemistry Environment Basis Set Database, version 1.2.2, as developed and distributed by the Molecular Science Computing Facility, Environmental and Molecular Sciences Laboratory, which is part of the Pacific Northwest Laboratory, P.O. Box 999, Richland, WA 99352, and funded by the U.S. Department of Energy.

(21) Ephritikhine, M. *Organometallics* **2013**, *32*, 2464–2488 and references cited therein.

(22) Evans, W. J.; Nyce, G. W.; Forrestal, K. J.; Ziller, J. W. *Organometallics* **2002**, *21*, 1050–1055.

(23) Evans, W. J.; Kozimor, S. A.; Ziller, J. W.; Kaltsoyannis, N. *J. Am. Chem. Soc.* **2004**, *126*, 14533–14547.

(24) Evans, W. J.; Traina, C. A.; Ziller, J. W. *J. Am. Chem. Soc.* **2009**, *131*, 17473–17481.

(25) Thomson, R. K.; Graves, C. R.; Scott, B. L.; Kiplinger, J. L. *Eur. J. Inorg. Chem.* **2009**, 2009, 1451–1455.

(26) Nutt, W. R.; Wells, R. L. *Inorg. Chem.* **1982**, *21*, 2469–2473.

(27) Bain, G. A.; Berry, J. F. *J. Chem. Educ.* **2008**, *85*, 532–536.